The EMBO Journal (2009) 28, 2042–2052 | © 2009 European Molecular Biology Organization | All Rights Reserved 0261-4189/09
www.embojournal.org

THE EMBO JOURNAL

Site-specific binding of a PPR protein defines and stabilizes 5′ and 3′ mRNA termini in chloroplasts

Jeannette Pfalz[1], Omer Ali Bayraktar, Jana Prikryl and Alice Barkan*

Institute of Molecular Biology, University of Oregon, Eugene, OR, USA

Chloroplast mRNA populations are characterized by overlapping transcripts derived by processing from polycistronic precursors. The mechanisms and functional significance of these processing events are poorly understood. We describe a pentatricopeptide repeat (PPR) protein, PPR10, whose binding defines mRNA segments derived from two transcription units in maize chloroplasts. PPR10 interacts *in vivo* and *in vitro* with two intergenic RNA regions of similar sequence. The processed 5′ and 3′ RNA termini in these regions overlap by approximately 25 nucleotides. The PPR10-binding sites map precisely to these overlapping sequences, and PPR10 is required specifically for the accumulation of RNAs with these termini. These findings show that PPR10 serves as a barrier to RNA decay from either the 5′ or 3′ direction and that a bound protein provides an alternative to an RNA hairpin as a barrier to 3′ exonucleases. The results imply that protein 'caps' at both 5′ and 3′ ends can define the termini of chloroplast mRNA segments. These results, together with recent insights into bacterial RNA decay, suggest a unifying model for the biogenesis of chloroplast transcript populations and for the determinants of chloroplast mRNA stability.

The EMBO Journal (2009) **28,** 2042–2052. doi:10.1038/emboj.2009.121; Published online 7 May 2009
Subject Categories: RNA; plant biology
Keywords: mitochondria; pentatricopeptide repeat; plastid; RNA-binding protein; RNA stability

Introduction

The chloroplast has retained many properties of its cyanobacterial ancestor, including operon-like polycistronic transcription units and an RNA polymerase that is closely akin to that in bacteria. However, the transfer of many endosymbiont genes encoding components of the photosynthetic apparatus to the nucleus, and the incorporation of the organelle into plants with distinct developmental stages and cell types necessitated the evolution of mechanisms to coordinate the activities of the nuclear and chloroplast genomes. Nucleus-encoded proteins that modulate chloroplast gene expression provide one means to this end. Several hundred such proteins are anticipated based on the current data, some of bacterial ancestry and others derived from the host genome. Prominent among the latter class are members of the pentatricopeptide repeat (PPR) family (Small and Peeters, 2000). PPR proteins are defined by degenerate 35 amino acid repeats that are related to the tetratricopeptide repeat (TPR). Genetic data have implicated PPR proteins in various aspects of organellar RNA metabolism in all eukaryotic lineages (reviewed in Schmitz-Linneweber and Small, 2008), but their mechanisms of action are poorly understood.

The results presented here define precise RNA-binding sites for a chloroplast PPR protein, and link binding at those sites to RNA stabilization and the accumulation of specific processed mRNA isoforms. Chloroplast RNA turnover (reviewed in Bollenbach *et al*, 2007) is believed to be initiated by endonucleolytic cleavage, followed by 3′-polyadenylation of the cleavage products and 3′→5′ exonucleolytic degradation. RNA hairpins at 3′ termini impede the 3′→5′ exonucleases, thereby stabilizing upstream RNA. This scenario is similar to that proposed for *Escherichia coli* (reviewed in Condon, 2007). Superimposed on this model is the notion that site-specific intercistronic cleavages generate the complex RNA populations that are characteristic of polycistronic transcription units in land plant chloroplasts (reviewed in Bollenbach *et al*, 2007).

In this context, several observations have been puzzling. First, the downstream products of endonucleolytic cleavage are rapidly degraded *in vivo* (reviewed in Bollenbach *et al*, 2007), suggesting that 5′ terminal features are important for stabilizing chloroplast mRNAs. This notion is supported by the analysis of chimeric genes in tobacco chloroplasts (Eibl *et al*, 1999) and by genetic data from *Chlamydomonas reinhardtii* (Boudreau *et al*, 2000; Vaistij *et al*, 2000a; Murakami *et al*, 2005; Loiselay *et al*, 2008). Second, in one of the few instances in which both the 5′ and 3′ termini of adjacent processed chloroplast RNAs have been mapped, the RNAs overlap in a manner that is not compatible with their biogenesis through a single cleavage event (Barkan *et al*, 1994).

The results presented here provide evidence for a conceptually simple mechanism that can account for these and other disparate observations. These insights emerged from the analysis of a maize PPR protein dubbed PPR10. We present evidence that PPR10 stabilizes two sets of chloroplast transcripts: RNAs with a 5′- or 3′-end mapping in either the *atpI-atpH* or *psaJ-rpl33* intergenic region. We show that bound PPR10 defines the positions of the 5′ and 3′ termini of processed transcripts derived from both regions, and that it substitutes for a 3′-terminal hairpin to protect upstream RNA from 3′ exonucleases. These and other findings suggest that protein 'caps' at 5′ and 3′ termini may be a major mechanism for defining chloroplast transcript populations. When considered in the context of recent advances in understanding RNA decay in bacteria, these results suggest revised models for the biogenesis of complex chloroplast transcript populations and for the determinants of chloroplast mRNA stability.

*Corresponding author. Institute of Molecular Biology, University of Oregon, Eugene, OR 97403, USA. Tel.: +1 541 346 5145; Fax: +1 541 346 5891; E-mail: abarkan@uoregon.edu
[1]Present address: Friedrich-Schiller-University, Jena, Germany

Received: 22 January 2009; accepted: 26 March 2009; published online: 7 May 2009

Results

PPR10 is required for chloroplast development

PPR10 belongs to the 'P' subfamily of PPR proteins, whose members lack additional domains (Schmitz-Linneweber and Small, 2008). Rice and Arabidopsis PPR10 orthologs (Os05g19380 and At2g18940, respectively) were identified through phylogenetic analyses (Supplementary Figure 1). PPR10 orthologs are predicted to begin with a chloroplast transit peptide, followed by approximately 100 amino acids and then 18 or 19 PPR motifs (Supplementary Figure 2). However, the SCOP server (Tung and Yang, 2007) and structural modelling of PPR10 (Supplementary Figure 3) predict that the N-terminal region also adopts a TPR-like structure. Therefore, virtually the entire mature portion of PPR10 is likely to consist of helical hairpin units.

We recovered two mutant alleles of *ppr10* in a reverse-genetic screen of our collection of transposon-induced non-photosynthetic maize mutants. Both insertions disrupt the open reading frame (Figure 1A) and cosegregate with mutations conferring a yellow-green seedling phenotype (Figure 1B). The progeny of crosses between *ppr10-1/+* and *ppr10-2/+* segregate yellow-green seedlings, showing lack of complementation between the alleles. Heteroallelic progeny of complementation crosses (*ppr10-1/-2*) were used in all phenotypic assays to ensure that the phenotypes result from disruption of *ppr10*. The mutant seedlings die after the development of three leaves, as is typical of non-photosynthetic maize mutants. The mutants have reduced levels of subunits of several photosynthetic enzyme complexes (Figure 1C); the AtpF subunit of CF_0 (the membrane-intrinsic portion of the ATP synthase) is the most severely reduced of the proteins assayed.

Polyclonal antibodies were raised against a PPR10 segment that lacks similarity to non-orthologous proteins. This antibody detects a protein of the size expected for mature PPR10 (~80 kDa) in wild-type leaf; this protein is absent in *ppr10* mutants (Figure 1D), verifying that it is PPR10.

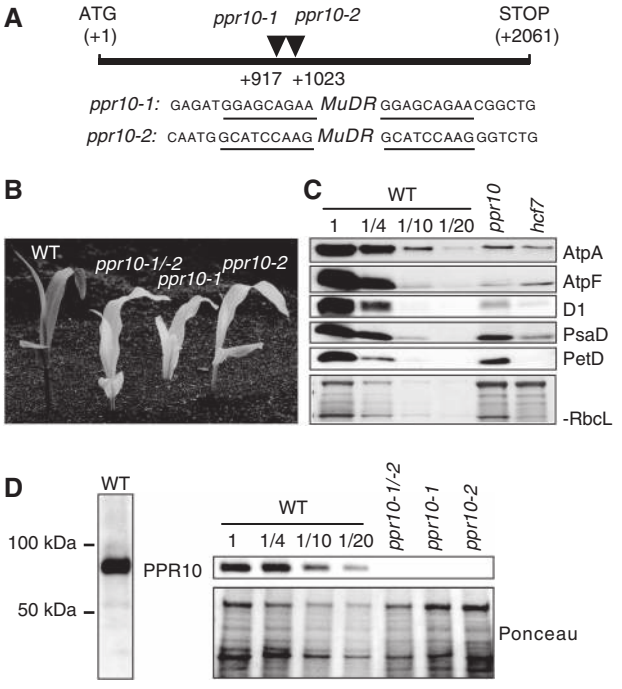

Figure 1 *ppr10* mutants. (**A**) Transposon insertions in *ppr10*. The PPR10 coding region is indicated by a rectangle. Sequences flanking the insertions are shown below with the target-site duplications underlined. Polymorphisms in the terminal inverted repeats identify the insertions as related to the MuDR member of the *Mu* family. (**B**) Phenotypes of *ppr10* mutants. Seedlings were grown for 8 days in soil. *ppr10-1/-2* is the progeny of a complementation cross. (**C**) Immunoblot analysis of photosynthetic complex subunits. Immunoblots of leaf extracts were probed with antibodies to proteins indicated to the right; the Ponceau S-stained blot below illustrates sample loading and the abundance of RbcL, the large subunit of Rubisco. AtpA and AtpF are subunits of the CF_1 and CF_0 portions of the ATP synthase, respectively. D1, PsaD and PetD are subunits of photosystem II, photosystem I and the cytochrome b_6f complex, respectively. *hcf7* illustrates protein losses resulting from a global decrease in plastid translation (Barkan, 1993). (**D**) Immunoblot detection of PPR10 in leaf extract, showing antibody specificity and loss of PPR10 in *ppr10* mutants. A full-colour version of this figure is available at *The EMBO Journal* Online.

PPR10 is associated with atpH and psaJ RNAs in chloroplast extract

Immunoblot analysis of leaf and subcellular fractions showed PPR10 to be enriched in isolated chloroplasts, where it was found solely in the stroma (Figure 2A). When stromal extract

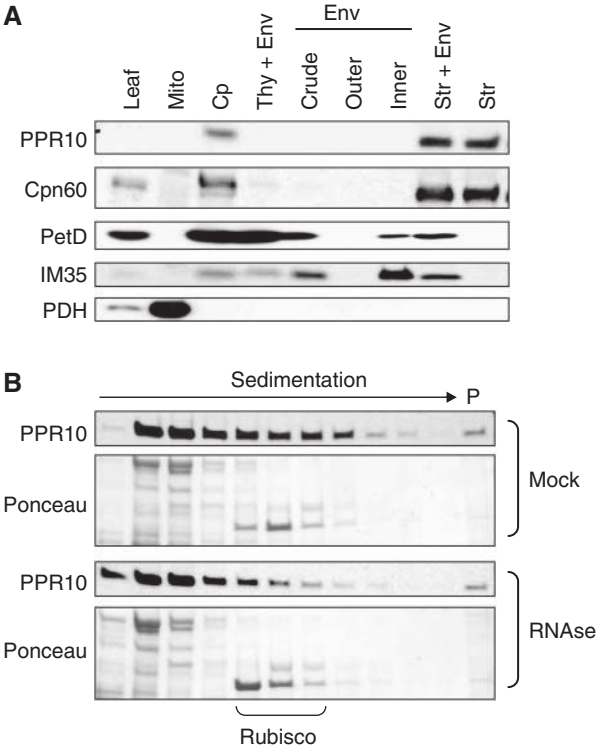

Figure 2 PPR10 is localized to the chloroplast stroma. (**A**) Immunoblots of leaf and subcellular fractions. Chloroplast (Cp) subfractions were loaded on the basis of equal chloroplast number. Replicate blots were probed with antibodies to the proteins indicated at left. Cpn60, PetD, IM35 and PDH were used as markers for stroma (Str), thylakoid (Thy), envelope (Env) and mitochondria (Mito), respectively. (**B**) Size distribution of PPR10-containing particles. Stroma was incubated with ribonuclease A (RNAse) or mock-treated and fractionated by sedimentation through sucrose gradients. An equal volume of each gradient fraction was analysed by probing immunoblots with PPR10 antibody. The Ponceau S-stained blots illustrate the position of Rubisco (~550 kDa). P, pelleted material.

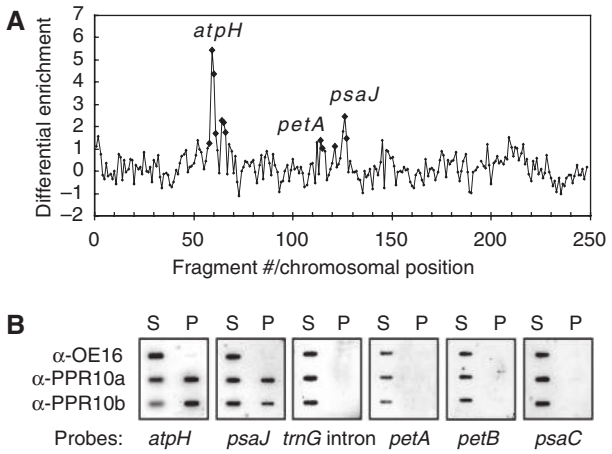

Figure 3 Coimmunoprecipitation assays identifying RNAs associated with PPR10. (**A**) Summary of RIP-chip data. The median $\log_2$-transformed enrichment ratios (F635/F532) for two replicate PPR10 immunoprecipitations are plotted according to chromosomal position after subtracting the corresponding values for a control immunoprecipitation with OE16 antibody. Data points that show significant differential enrichment between the PPR10 and control assays (*P*-value <1E-4) are marked with diamonds and are annotated with the locus name. The underlying data for the highest-ranking fragments are summarized in Supplementary Table 1. (**B**) Validation of RIP-chip data. Immunoprecipitations were performed as for RIP-chip assays except that ribonuclease inhibitor was not included. One-sixth of the RNA from each immunoprecipitation pellet (P) and one-twelfth of the RNA from the corresponding supernatant (S) were applied to replicate slot blots. The two PPR10 immunoprecipitations (a and b) used sera from different immunized rabbits. Blots were probed with oligonucleotides specific for the *atpH* 5′ UTR, the *psaJ* 3′ UTR, the *petA* 5′ UTR and the coding regions of the other genes indicated.

was fractioned by sedimentation through a sucrose gradient, PPR10 was found in a broad peak representing particles between ~100 and 600 kDa (Figure 2B). Treatment of the extract with ribonuclease shifted the PPR10 distribution toward smaller particles, suggesting that a fraction of PPR10 is associated with RNA.

We used a 'RIP-Chip' assay as an initial screen to identify the RNAs that associate with PPR10 in chloroplast extract: RNAs purified from the pellets and supernatants of PPR10 immunoprecipitations were labelled with a red-fluorescing or green-fluorescing dye, respectively, combined and hybridized to a tiling microarray of the maize chloroplast genome (Schmitz-Linneweber *et al*, 2005). Two replicate experiments were performed, using PPR10 antibodies from different immunized rabbits. An immunoprecipitation with antiserum to OE16 served as a negative control. Figure 3A shows the median enrichment ratio for each array element plotted as a function of chromosomal position, after subtracting the corresponding values for the control assay. The most highly significant peaks represent sequences near the *atpH* and *psaJ* loci. Within these peaks, the strongest enrichment was detected near the 5′ end of *atpH* and the 3′ end of *psaJ*. Slot-blot hybridization of immunoprecipitated RNAs validated the specific enrichment of *atpH* 5′ UTR and *psaJ* 3′ UTR RNA sequences in PPR10 immunoprecipitations (Figure 3B). RNA from near the *petA* locus appeared to be enriched by RIP-chip, but did not reproduce in the slot-blot assay. These results point to RNAs from the 5′ region of *atpH* and the 3′ region of *psaJ* as the primary and possibly the sole physiological ligands of PPR10.

Fine-mapping coimmunoprecipitated RNAs reveals a consensus sequence at sites of PPR10 association

To precisely map the RNA sequences that are associated with PPR10, immunoprecipitations were performed without ribonuclease inhibitor so as to decrease the size of the coimmunoprecipitated RNA fragments. RNAs recovered from the immunoprecipitation pellets and supernatants were applied to slot-blots and hybridized to a series of 60-nt probes from the *atpH* and *psaJ* loci (Figure 4). The strongest enrichment at the *atpH* locus was detected with the *atpH*-2 60-mer (Figure 4A); the strongest enrichment at the *psaJ* locus was detected with the *psaJ*-5 60-mer (Figure 4B). An alignment of sequences in these regions (Figure 4C) revealed strong sequence similarity spanning approximately 30 nucleotides. Experiments described below showed that this shared sequence is directly recognized by PPR10.

PPR10 is required for the accumulation of RNAs with a 5′- or 3′-end mapping to sites of PPR10 interaction

To investigate the role of PPR10, chloroplast RNA in *ppr10* mutants was initially profiled by hybridization to our chloroplast tiling microarray (Supplementary Figure 4). The results suggested that *ppr10* mutants have reduced levels of *atpH* and *psaJ* RNAs, correlating with the finding that these are PPR10 ligands. RNA gel blots were used to validate and extend these findings (Figure 5). *hcf7* mutants, which have a global decrease in chloroplast translation (Barkan, 1993), were analysed in parallel to control for indirect effects resulting from compromised photosynthesis. The results showed that *ppr10* mutants lack specific transcripts from both the *atpH* and *psaJ* transcription units. Other transcripts suggested by either the RIP-chip data or microarray RNA profile to be PPR10 targets were also examined by RNA gel blot hybridization (Supplementary Figure 5); the abundance of *petA* RNA is reduced slightly in *ppr10* mutants, but no other differences were detected between *ppr10* and the control *hcf7* mutants.

The *atpH* and *psaJ* transcript data revealed a striking correspondence between those RNAs that are absent in *ppr10* mutants and those with termini mapping near PPR10's *in vivo* interaction sites. Thus, all transcripts with a 5′- or a 3′-end mapping in either the *atpH -atpI* (Figure 5A) or the *psaJ-rpl33* (Figure 5B) intergenic region fail to accumulate in *ppr10* mutants (transcripts in grey). The positions of the termini of PPR10-dependent transcripts were estimated by probing blots with the 60-mers used to fine-map the coimmunoprecipitating RNAs. The atpH-2 60-mer hybridized to the PPR10-dependent *atpH* transcripts, whereas the adjacent atpH-3 60-mer did not (Figure 5A). A primer extension assay placed this 5′ end approximately 46 nucleotides upstream of the *atpH* start codon (Figure 6A), consistent with the RNA gel blot data and with an earlier report of a 5′ end near this position (Stahl *et al*, 1993). The psaJ-5 60-mer hybridized to PPR10-dependent *psaJ* transcripts, whereas the adjacent psaJ-6 60-mer did not (Figure 5B); this placed the 3′ end of PPR10-dependent *psaJ* RNAs near the 'downstream' end of the psaJ-5 sequence. Together, the genetic and coimmunoprecipitation data indicate that PPR10 is bound very near the termini of the transcripts that fail to accumulate in its

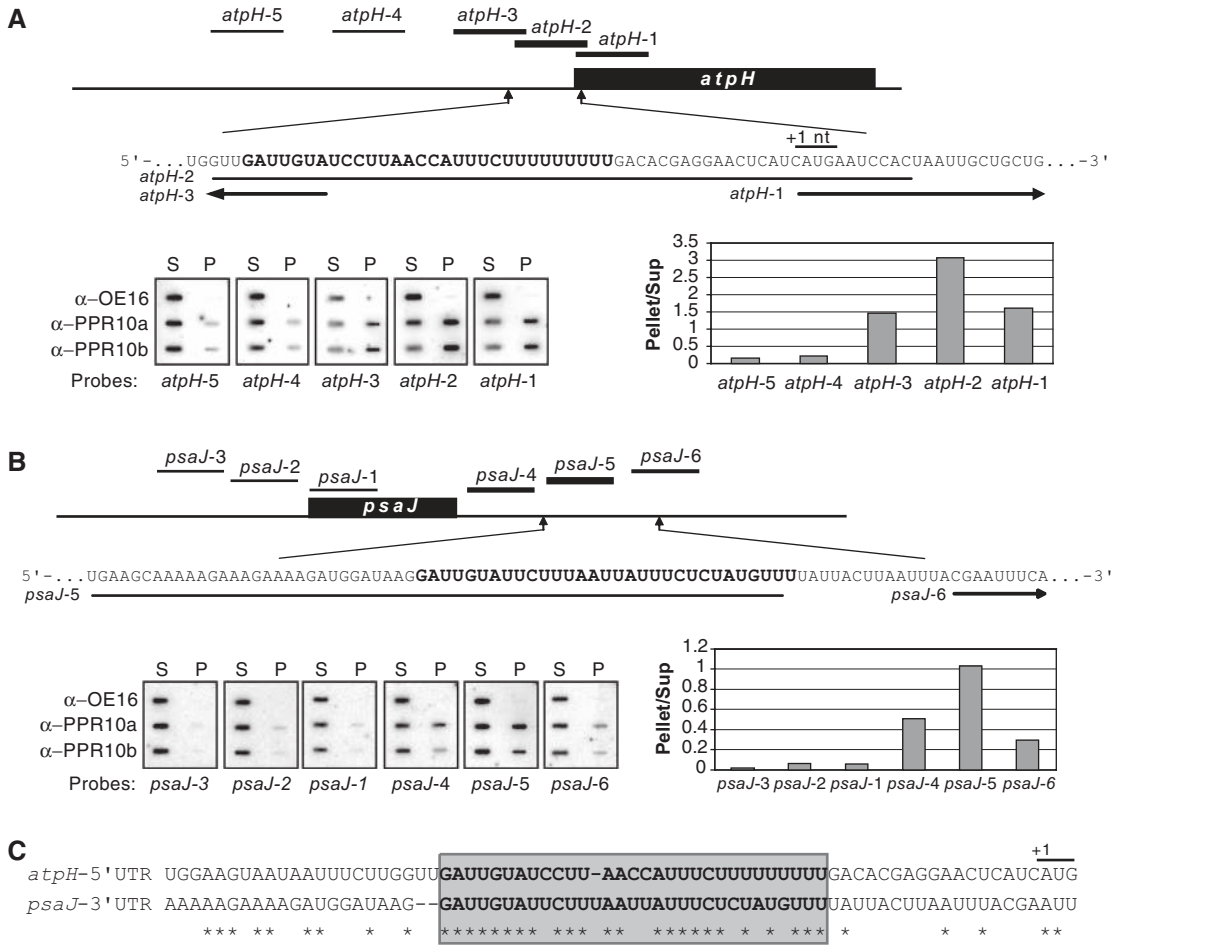

Figure 4 Fine-mapping RNAs that coimmunoprecipitate with PPR10. (**A**, **B**) Replicate slot blots were prepared from immunoprecipitation pellet (P) and supernatant (S) RNAs, as described in Figure 3B. The positions of the 60-mer oligonucleotide probes are diagrammed, using line weights that reflect the degree to which corresponding RNAs were enriched in PPR10 immunoprecipitations. The most strongly enriched sequences are shown below, with the consensus residues shared by the *atpH* and *psaJ* sites highlighted in bold. The data were quantified with a phosphorimager, and are graphed at right. (**C**) Alignment of sequences near *atpH* and *psaJ* that coimmunoprecipitate with PPR10, with the consensus highlighted.

absence. The loss of processed RNAs in *ppr10* mutants was not accompanied by an increased abundance of precursor transcripts, arguing that transcript loss is caused by transcript instability rather than by a defect in precursor cleavage.

Phosphorimager analysis of the RNA gel blot data showed that the total abundance of *atpH* transcripts is reduced by approximately three-fold in *ppr10* mutants (data not shown). This is insufficient to account for the >10-fold decrease in the abundance of the CF_0 complex (as monitored by its AtpF subunit in Figure 1C), suggesting that PPR10 might enhance the translation of the *atpH* ORF. To address this possibility, we examined the association of *atpH* mRNAs with polysomes (Supplementary Figure 6). The residual *atpH* transcripts in the *ppr10* mutant were shifted toward polysomes of smaller size, consistent with a translation-enhancing role for PPR10. However, the polycistronic nature of these RNAs precludes firm conclusions. In fact, these data suggested a small global decrease in plastid translation in *ppr10* mutants, consistent with their moderate reduction in all photosynthetic enzyme complexes harbouring plastid-encoded subunits (Figure 1C).

Overlapping transcript termini in the atpI-atpH and psaJ-rpl33 intergenic regions highlight PPR10 interaction sites

To obtain more comprehensive information about the termini of PPR10-dependent transcripts, transcript termini in the *atpI-atpH* and *psaJ-rpl33* intergenic regions were determined by circularization RT–PCR (cRT–PCR) (Figure 6B; Supplementary Table 2). The results showed that the adjacent processed RNAs in both regions overlap in a manner that is not compatible with their biogenesis through a single endonucleolytic cleavage (Figure 6C). Strikingly, the length of the overlap between the most abundant transcript isoforms is almost identical in the two regions (24–25 nts) (Figure 6C), and this overlap lies entirely within the consensus sequence shared by the RNAs that most strongly coimmunoprecipitate with PPR10. These results together with the genetic and RNA gel blot data strongly suggest that PPR10 is associated *in vivo* with the termini of the overlapping transcripts in both intergenic regions, and that this interaction is necessary to stabilize the processed transcripts.

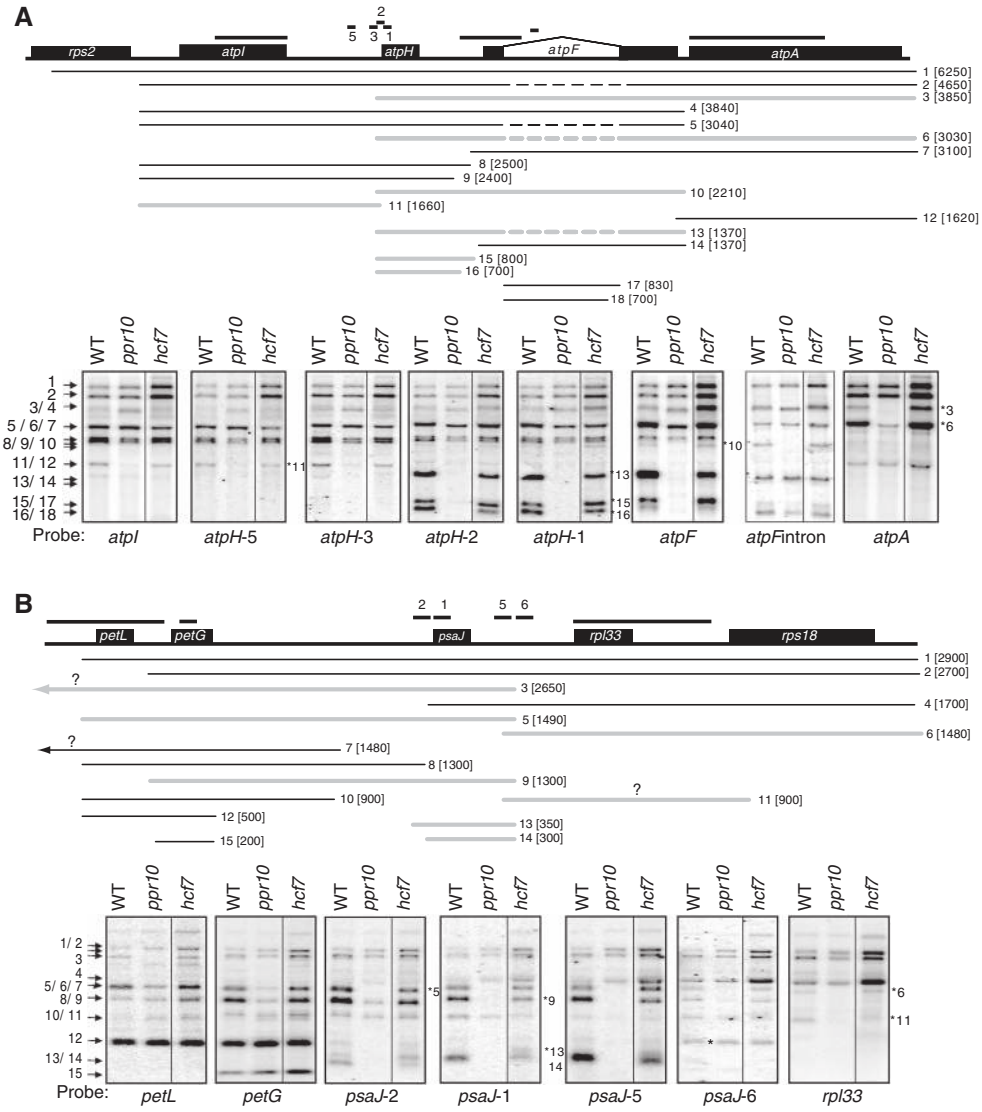

Figure 5 RNA gel blot analysis of *atpH* (**A**) and *psaJ* (**B**) RNAs in *ppr10* mutants. Probes are diagrammed above the maps as black lines. Numbered probes correspond to the same 60-mer oligonucleotides used for slot blot hybridizations in Figure 4. Transcript maps were generated based on transcript size, the probes with which they hybridized and by the cRT–PCR data in Supplementary Table 2. RNAs missing in *ppr10* mutants are in grey. Dashed lines indicate the spliced *atpF* intron. The band marked with an asterisk on the *psaJ*-6 blot derives from a prior probing with the *petG* probe. These transcript maps are consistent with and expand on those reported earlier (Stahl *et al*, 1993; Miyagi *et al*, 1998; Yamazaki *et al*, 2004); remaining ambiguities are indicated with question marks. All lanes in each panel come from the same gel.

Recombinant PPR10 binds with specificity to the consensus sequence in the atpH 5′-UTR and psaJ-3′ UTR

The above results highlight the 'consensus' sequences shared by the overlapping PPR10-dependent RNA termini in the *atpI-atpH* and *psaJ-rpl33* regions as potential PPR10-binding sites. To test whether PPR10 directly binds these sequences, *in vitro* assays were performed with purified recombinant PPR10 (rPPR10). rPPR10 has a monomeric molecular weight of 79 kDa, but eluted from a size-exclusion column at a position corresponding to a globular protein of ~160 kDa, suggesting that it forms a homodimer (Figure 7A). Preliminary analytical ultracentrifugation data support this interpretation (data not shown), but we cannot eliminate the possibility that rPPR10 is a highly elongated monomer.

Gel mobility shift assays were performed with rPPR10 and synthetic RNAs of ~30 nts (Figure 7B and C). rPPR10 bound with high affinity to RNAs containing the sequences shared by the overlapping termini in the *atpI-atpH* and *psaJ-rpl33* intergenic regions, but did not bind to RNAs of the same length containing sequences from nearby regions. Under the assay conditions used here (RNA concentration well below the K_d and protein in excess), the K_d can be estimated as the protein concentration at which half of the RNA is bound. Thus, the K_d for the interaction between rPPR10 and the *atpH* 30-mer is <10 nM. These results indicate that PPR10 is an RNA-binding protein that binds with high specificity and affinity to sequences shared at the termini of transcripts whose accumulation it promotes.

Discussion

The results presented here elucidate how a PPR protein modulates gene expression and the factors that determine the termini and stability of chloroplast mRNAs. We show that

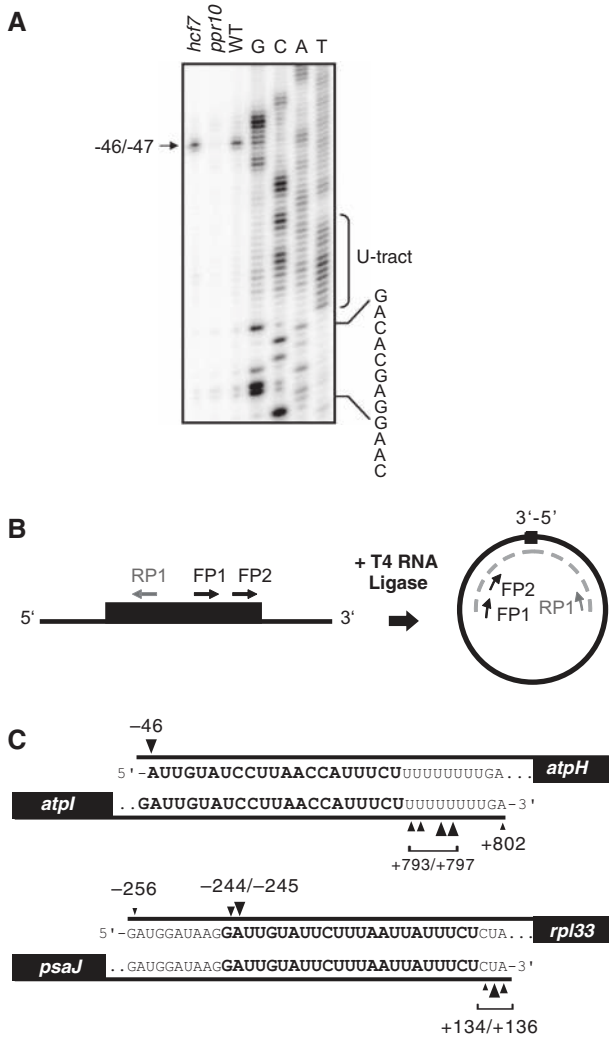

Figure 6 Positions of PPR10-dependent RNA termini. (**A**) Primer extension mapping of the PPR10-dependent *atpH*-5′ end. A sequencing ladder generated with the same primer on an *in vitro* transcript is shown to the right. The U-tract disrupts the fidelity of reverse transcriptase, making the distal sequence ambiguous. (**B**) cRT–PCR procedure used to map transcript termini. Primer RP1 was used for reverse transcription. PCR was performed initially with RP1 and FP1 primers; nested PCR was then performed with RP1 and FP2. (**C**) Overlapping transcript termini in the *atpI/atpH* and *psaJ/rpl33* intergenic regions. Residue numbers refer to position relative to the start codons of *atpH* and *rpl33* or the stop codons of *atpI* and *psaJ*. Triangle size reflects relative transcript frequency, based on the data in Supplementary Table 2. Residues that are most highly conserved between the two sites are highlighted.

PPR10 is a sequence-specific RNA-binding protein that binds *in vivo* and *in vitro* to RNAs from two genomic regions of similar sequence. PPR10 binds the immediate 5′ or 3′ termini of RNAs that accumulate in a PPR10-dependent manner, indicating that PPR10 defines the positions of these termini and is required for the accumulation of RNAs harbouring them. The simplest explanation of our results is that bound PPR10 serves as a protective 'cap' to stabilize upstream and downstream RNA by blocking exonucleases from both the 5′ and 3′ directions. The loss of processed transcripts in *ppr10* mutants with no accompanying increase in their precursors argues for a defect in RNA stabilization rather than a defect in precursor cleavage. Furthermore, the results are not consistent with a role for PPR10 in promoting simple endonucleolytic cleavages because the overlapping 5′ and 3′ PPR10-dependent termini in each region are not products of a single cleavage event.

An RNA stabilization function for PPR10 is compatible with evidence that two other PPR proteins directly protect RNA from nucleases. Genetic data support a model in which MCA1 in *C. reinhardtii* binds to the 5′ terminal ~21 nucleotides of chloroplast *petA* mRNA and protects the downstream RNA from degradation (Loiselay *et al*, 2008). Biochemical and genetic experiments showed that maize PPR5 stabilizes a chloroplast tRNA precursor by binding to an endonuclease-sensitive site within its intron (Beick *et al*, 2008; Williams-Carrier *et al*, 2008). The results with PPR10 add to this picture by providing evidence that a bound PPR protein (1) can block 5′→3′ degradation of chloroplast RNAs in a land plant and (2) can protect upstream RNA from 3′→5′ exonucleases. Taken together, these findings provide strong evidence that a bound PPR protein can directly block the cleavage of chloroplast RNAs from the 5′ direction, from the 3′ direction and from internal endonucleolytic attack.

The conclusion that a bound PPR protein can protect both upstream and downstream RNA from degradation was foreshadowed by prior studies. The PPR protein CRP1 is required for the accumulation of processed transcripts with a 5′- or 3′-end mapping between the *petB* and *petD* loci in maize chloroplasts (Barkan *et al*, 1994; Fisk *et al*, 1999). The CRP1-dependent termini overlap by approximately 30 nucleotides, and the loss of the processed isoforms in *crp1* mutants is not accompanied by an increased level of precursors (Barkan *et al*, 1994). In light of the current findings, a reasonable hypothesis is that CRP1 (or a CRP1-dependent partner) stabilizes both the upstream and downstream processed RNAs by binding their overlapping sequence. Although interactions between CRP1 and the *petB/petD* intergenic RNA were not unambiguously detected in RNA coimmunoprecipitation assays (Schmitz-Linneweber *et al*, 2005), we suspect that heterodimerization of CRP1 may mask the CRP1 epitope in *petB/D* ribonucleoprotein particles (unpublished results).

The PPR protein HCF152 may also function analogously to PPR10. Arabidopsis *hcf152* mutants lack chloroplast transcripts with either a 5′- or 3′-end mapping between the *psbH* and *petB* loci, again with no increase in uncleaved precursors (Meierhoff *et al*, 2003). To explore this possibility, we mapped RNA termini in the *psbH/petB* intergenic region in maize (Supplementary Figure 8); indeed, the processed *psbH* and *petB* termini overlap by approximately 20 nucleotides. In light of the other results presented here, it seems likely that this overlap represents the HCF152-binding site and that the *hcf152* phenotype results from the 'uncapping' of the upstream and downstream RNA sequences.

Interlinked RNA processing, RNA stabilization and translation in chloroplasts

A dual role in RNA stabilization and translational enhancement has been proposed for several PPR-like proteins in chloroplasts (Barkan *et al*, 1994; Felder *et al*, 2001; Yamazaki *et al*, 2004; Loiselay *et al*, 2008). The magnitude of the CF_0 deficiency in *ppr10* mutants (Figure 1) and polysome data (Supplementary Figure 6) hint that PPR10, in addition to stabilizing *atpH* mRNA, also stimulates *atpH* translation. The position of the PPR10-binding site suggests

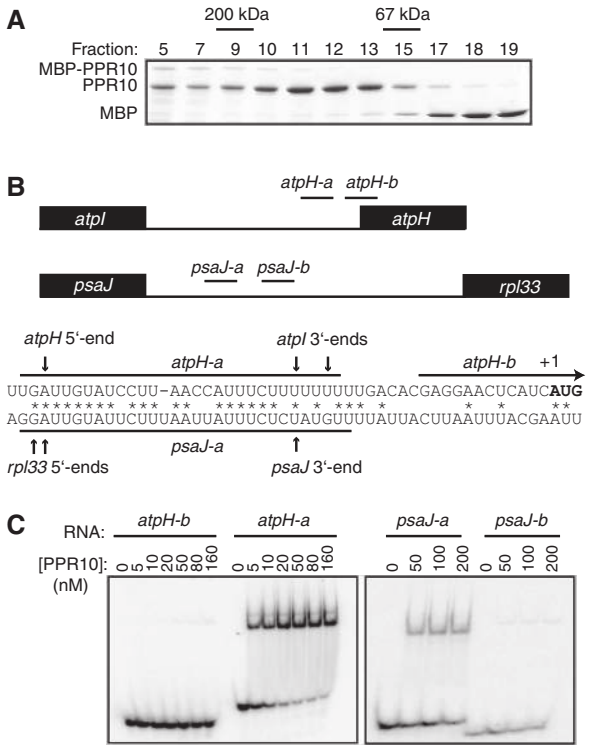

Figure 7 rPPR10 binds with specificity to the consensus sequences shared by the *atpH* 5′ UTR and *psaJ* 3′ UTR. (**A**) Elution of rPPR10 from a size-exclusion column. Column fractions were fractionated by SDS–PAGE and stained with Coomassie blue. The elution positions of β-amylase (200 kDa) and BSA (67 kDa) are shown. Fractions 10, 11 and 12 were pooled for binding assays. (**B**) RNA oligonucleotides used for binding assays. The *atpH-a* and *psaJ-a* sequences are shown below, aligned according to their consensus sequence. The positions of mapped RNA termini (see Figure 6) are marked with arrows. (**C**) Gel mobility shift assays. Binding reactions contained RNA at100 pM and the indicated concentration of rPPR10. The control RNAs (*atpH-b* and *psaJ-b*) were matched to the corresponding RNAs in length but migrated differently due to distinct structures.

a mechanism for this link. It seems likely that PPR10 bound to the *atpH* 5′ UTR spans the overlap between the upstream and downstream processed transcripts, which we believe represents an *in vivo* PPR10 'footprint'. Thus, the downstream edge of PPR10 is likely to be very near position −20 with respect to the *atpH* start codon (see Figure 7B). As 70S ribosomes span ∼15 nts on each side of the start codon (Steitz and Jakes, 1975), bound PPR10 must be very close to initiating ribosomes. Thus, PPR10 might enhance translation by contacting initiating ribosomes or by maintaining the ribosome-binding site in single-stranded form through sequestration of adjacent RNA. This latter possibility is especially appealing because the putative Shine-Dalgarno site is paired with the PPR10-binding site in the predicted secondary structure of the *atpH* 5′ UTR (Supplementary Figure 7). The translation enhancing effects of several RNA processing/stabilization factors in chloroplasts have been suggested to result from their role in producing RNA isoforms that are inherently more translatable than their precursors (e.g. Barkan *et al*, 1994; Felder *et al*, 2001); this scenario is also plausible in the case of the PPR10-dependent *atpH* RNAs. However, an alternative interpretation is that it is the presence of these proteins at the processed 5′ termini that enhances translation.

The *ppr10* mutants exhibit a modest global reduction in plastid translation. A similar observation was made for *crs1* mutants, which lack the CF_0 complex due to a defect in *atpF* intron splicing (Till *et al*, 2001). The *ppr10* mutants likewise lack the CF_0 complex, albeit due to a defect in expression of the AtpH subunit. This commonality suggests that the absence of CF_0 might underlie the mild global translation defect in both *crs1* and *ppr10* mutants.

PPR proteins as determinants of stable 5′ and 3′ chloroplast mRNA termini

There is extensive genetic evidence that proteins bound in 5′ UTRs can protect downstream RNA from degradation in Chlamydomonas chloroplasts (Drager *et al*, 1998, 1999; Nickelsen *et al*, 1999; Boudreau *et al*, 2000; Vaistij *et al*, 2000b; Murakami *et al*, 2005; Loiselay *et al*, 2008). Strong support for the existence of an analogous mechanism in plants has been lacking (Bollenbach *et al*, 2007), although the phenotypes of various mutants were suggestive (Barkan *et al*, 1994; Felder *et al*, 2001; Lezhneva and Meurer, 2004; Yamazaki *et al*, 2004; Sane *et al*, 2005). It has also been unclear whether net RNA degradation in the 5′→3′ direction is accomplished by a 5′→3′ exonuclease or through vectorial cleavage by an endonuclease, largely because a candidate for a 5′→3′ exonuclease in chloroplasts has been lacking (Bollenbach *et al*, 2007). The results presented here, together with recent progress in understanding RNA decay in bacteria, clarify these issues. Recently, it was discovered that RNAse J in *Bacillus subtilis*, long considered to be strictly an endonuclease, also has 5′→3′ exonuclease activity (Mathy *et al*, 2007). This led to a revision in the view that RNA decay in all bacteria follows the *E. coli* paradigm, where it is initiated by endonucleolytic cleavage followed by 3′→5′ exonucleolytic degradation (Condon, 2007). Cyanobacterial genomes and nuclear genomes in plants and algae encode an RNAse J homologue; this protein has been detected in chloroplasts (see http://ppdb.tc.cornell.edu/gene.aspx?acc = AT5G63420.1). Thus, RNAse J is an excellent candidate for the 5′→3′ exonuclease in chloroplasts whose existence has been suggested by genetic data. The fact that PPR10 is bound precisely at the 5′ termini of RNAs that fail to accumulate in its absence is most easily explained by a model in which PPR10 serves as a protective cap to block the activity of a 5′→3′ exonuclease. A reasonable scenario is that PPR10 and other chloroplast proteins that act through a 5′ UTR to stabilize downstream RNA block exonucleolytic degradation by chloroplast RNAse J (see Figure 8). Bound ribosomal subunits and strong 5′ RNA structures impede the progress of *B. subtilis* RNAse J (Mathy *et al*, 2007; Deikus *et al*, 2008). These features may also apply to the chloroplast enzyme, providing alternative mechanisms for protection of 5′ termini.

Protection of chloroplast RNAs from 3′→5′ exonucleases has been attributed to 3′ stem–loops (reviewed in Bollenbach *et al*, 2007). The results presented here indicate that a bound protein can serve as an alternate mechanism to block 3′ exonucleases. The PPR10-binding sites map at the immediate 3′ ends of those *atpI* and *psaJ* RNAs whose accumulation requires PPR10. An RNA stem–loop is not predicted for the *atpI* 3′ terminus or for the immediate *psaJ* 3′ end (Supplementary Figure 7). Furthermore, the strong preference of PPR proteins for single-stranded RNA (Williams-Carrier *et al*, 2008) suggests that PPR10 binding will disrupt

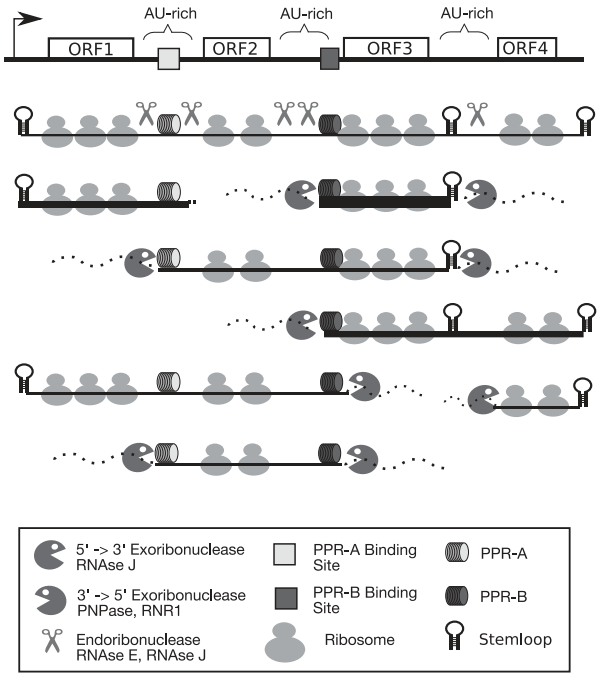

Figure 8 Model linking mechanisms for intercistronic RNA processing and differential mRNA stability in chloroplasts. In this model, intercistronic processing and RNA degradation are both initiated by endonucleolytic cleavage of AU-rich sequences that are not masked by RNA structure, ribosomes, or proteins. The cleaved products are substrates for 3′→5′ and 5′→3′ exonucleases, which proceed until blocked by a strong RNA structure or bound protein. The ribonucleolytic activities are proposed to reside in homologues of the bacterial enzymes indicated in the key. Protective functions are attributed here to PPR proteins, but other protein classes could function analogously. The relative accumulation of the different transcripts is indicated by line thickness. Transcript level is proposed to be determined primarily by the accessibility of the AU-rich targets for RNAses E and J in untranslated regions, which determines both the rate of processing and the stabilities of the processed products. For example, ORF3 mRNA is most abundant because the PPR-B-binding site abuts the ribosome-binding site and the 3′ UTR is short and structured. Only a subset of potential processed RNAs is shown. A full-colour version of this figure is available at *The EMBO Journal* Online.

any RNA structures that might otherwise form. Thus, the simplest explanation of our findings is that these 3′ termini are protected by bound PPR10. Protein-mediated protection might apply to many 3′ termini in chloroplasts (see Figure 8) and could apply to bacterial and mitochondrial RNA termini as well.

Implications for the biogenesis of complex transcript populations in land plant chloroplasts

Most genes in higher plant chloroplasts are transcribed as polycistronic RNAs that give rise to processed transcripts with termini mapping between coding regions. It has generally been assumed that this intercistronic RNA processing is accomplished by site-specific endonucleolytic cleavages. However, the overlapping termini shown here for the *atpI-atpH*, *psaJ-rpl33* and *psbH-petB* intergenic regions, and shown earlier for the *petB-petD* region (Barkan *et al*, 1994), are not consistent with biogenesis through a single cleavage in each region. Few processed 3′ termini in chloroplasts have been mapped with sufficient resolution to evaluate their conformity to this pattern. Ribonuclease-protection data for termini in the *psaC-ndhD* intergenic region (Hirose and Sugiura, 1997) and for the CRR2-dependent termini in the *rps7-ndhB* intergenic region (Hashimoto *et al*, 2003) are consistent with overlapping termini, but the resolution of these data are insufficient to make firm conclusions. In fact, we are aware of only one instance in which 5′ and 3′ termini within a chloroplast intergenic region have been unambiguously shown *not* to overlap in this manner (Hashimoto *et al*, 2003); in this case, the 'adjacent' termini are quite far apart and appear to arise from independent processing events.

We propose a substantially revised mechanism for the biogenesis of processed transcript populations in chloroplasts that is based on (1) the finding that PPR10 stabilizes specific chloroplast RNAs by capping both 5′ and 3′ termini; (2) the lack of evidence that highly specific endonucleolytic cleavages are generally responsible for intercistronic RNA processing and (3) results summarized above suggesting that chloroplasts have both 5′→3′ and 3′→5′ exonucleases. This model invokes no undocumented activities: it incorporates known features of bacterial homologues of chloroplast ribonucleases and established functions of PPR proteins. We suggest that processing is generally initiated by endonucleases with little sequence specificity, but that cleavage typically occurs in intercistronic regions simply because these regions are not masked by ribosomes. The resulting termini are substrates for 5′→3′ and 3′→5′ exonucleases. The 'mature' mRNA termini are then defined by the positions of bound proteins or RNA structures that block the exonucleases at discrete sites (Figure 8). We further suggest that the chloroplast RNAse E and RNAse J homologues act as the endonucleases that initiate these events, and that they target unstructured AU-rich sequences as they are suggested to do in bacteria (Cohen and McDowall, 1997; Deikus *et al*, 2008). AU-rich sequences are plentiful in chloroplast intergenic regions, so redundancy of the initial cleavage sites can be anticipated. These aspects of the model are consistent with the stabilizing effect of translating ribosomes in bacteria (Deana and Belasco, 2005; Dreyfus, 2009), the presence of an RNAse E homologue in chloroplasts (Mudd *et al*, 2008; Schein *et al*, 2008), the sequence preference this enzyme exhibits *in vitro* (Schein *et al*, 2008), and the fact that mutating an AU-rich sequence needed for 3′ processing of a chloroplast RNA *in vitro* did not alter the position of the 3′ end *in vivo* (Rott *et al*, 1999). Finally, we propose that chloroplast RNAse J functions not only as an endonuclease, but also as a 5′→3′ exonuclease, as it does in *B. subtilis*. The 3′→5′ exonucleolytic activities presumably reside in the various exonucleases of prokaryotic origin earlier implicated in chloroplast RNA decay (reviewed in Bollenbach *et al*, 2007). This model does not preclude the possibility that site-specific cleavages contribute to processed RNA populations in some cases. For example, some members of the 'DYW' subfamily of PPR proteins may function in this manner (Hashimoto *et al*, 2003; Nakamura and Sugita, 2008).

A prediction of our model is the presence *in vivo* of short RNA segments representing minimal nuclease-resistant 'footprints' of bound PPR proteins. In fact, evidence for such molecules can be found among the small, non-coding RNAs reported in angiosperms. Small RNAs detected in tobacco chloroplasts (Lung *et al*, 2006) and in rice (Morin *et al*, 2008) match the sequence shared by the overlapping termini of the processed *psbH* and *petB* transcripts mapped here

(Supplementary Figure 8). The accumulation of RNAs with these termini requires the PPR protein HCF152 (Meierhoff *et al*, 2003). It seems likely that this small RNA is actually the *in vivo* HCF152 footprint, although it does not correspond to the binding sites proposed on the basis of *in vitro* cross-linking experiments (Nakamura *et al*, 2003). Another small RNA detected in tobacco chloroplasts and in rice (Lung *et al*, 2006; Morin *et al*, 2008) corresponds to the 5′ end of the processed chloroplast *ndhB* RNA that requires the PPR protein CRR2 for its accumulation (Hashimoto *et al*, 2003); this small RNA might represent the minimal CRR2 footprint. Queries of the Cereals Small RNAs Database (http://sundarlab.ucdavis.edu/smrnas/) revealed these and other putative PPR-binding sites as stand-alone small RNAs of approximately 20 nucleotides, including the PPR10-binding site itself (data not shown).

This model has implications for mechanisms that determine the stabilities of chloroplast mRNAs. Multiple parameters are likely to contribute to the determination of mRNA half-life, including the spacing between ribosomes, the fraction of time that RNA termini are protected by proteins or RNA structures and the activities of the ribonucleases that initiate decay. However, untranslated regions may typically be the sites of initiating endonucleolytic cleavages because they are not protected by ribosomes. Thus, the accessibility of AU-rich sequences to RNAse E/J cleavage in untranslated regions may be a key determinant of mRNA stability. The asymmetric accumulation of the upstream and downstream PPR10-dependent transcripts supports this notion (Figure 5). The *atpI* transcripts ending at the PPR10-binding site are found at low abundance, correlating with their long AU-rich 3′ UTR that may offer plentiful targets for RNAse E/J cleavage (modelled by the ORF2 mRNA in Figure 8). In contrast, *atpH* RNAs starting at the PPR10-binding site are found at high abundance, correlating with masking of the entire *atpH* 5′ UTR by PPR10 and the adjacent initiating ribosome (modelled by ORF3 mRNA in Figure 8). An analogous scenario applies in the *psaJ/rpl33* region: in this case, however, the upstream processed RNAs are more abundant, correlating with their short 3′ UTR, whereas the downstream processed *rpl33* mRNAs are less abundant correlating with their long, AU rich 5′ UTR. This model can explain the differential accumulation of RNA segments derived from the same polycistronic transcription unit. Thus, PPR10 binding may be responsible for the high ratio of RNA from *atpH* relative to *atpI*, *atpF* and *atpA* with which it is cotranscribed. These RNA ratios correlate with the stoichiometry of the corresponding proteins in the ATP synthase complex (Hotchkiss and Hollingsworth, 1997). Segmental expression within this and other polycistronic transcription units might be enhanced further by differential translation.

A widespread role for PPR proteins as mRNA 'caps'?

Genetic data summarized above are consistent with the possibility that other PPR-like proteins in chloroplasts define 5′ and 3′ RNA termini by blocking RNA degradation from both directions. Angiosperm chloroplast genomes encode approximately 80 proteins, most of which are represented by both monocistronic and polycistronic mRNAs. Given that characterized PPR proteins target one or several RNAs, it seems possible that this mechanistically simple but essential protective role can account for the functions of the majority of the approximately 100 predicted chloroplast PPR proteins in land plants that lack additional domains (O'Toole *et al*, 2008). The long RNA/protein interface predicted for PPR proteins seems particularly well suited to a capping function, as protection of the adjacent RNA will be maintained even during transient 'breathing' at the ends of the interface. Thus, this type of activity may apply also to PPR-like proteins found outside of chloroplasts and outside of the plant kingdom.

Materials and methods

Nucleic acids

A *ppr10* cDNA clone (Accession EE016216) was obtained from the Arizona maize cDNA project (http://www.maizecdna.org/). The sequence is deposited in GenBank under Accession FJ490677. The sequences of PCR primers, hybridization probes and RNA oligonucleotides are provided in Supplementary Table 3.

Plant material

Mutant *ppr10* alleles were identified in a reverse genetic screen of a collection of *Mu*-induced non-photosynthetic maize mutants (http://chloroplast.uoregon.edu) by amplification of pooled mutant DNAs with gene-specific and *Mu*-specific primers (Williams and Barkan, 2003). Plants were grown in soil under a 16-h light (28°C)/8-h dark (26°C) cycle and harvested between 7 and 9 days after planting. Phenotypic analyses used the *ppr10-1/-2* progeny of complementation crosses.

Antibody production

A PPR10 fragment (amino acids 46–168) with a C-terminal 6xhistidine tag was expressed from a pet28b(+) vector (Novagen). The antigen was purified from urea-solubilized inclusion bodies by nickel affinity chromatography as described earlier (Watkins *et al*, 2007). Antisera were generated at Quality Controlled Biochemicals. The antigen was used to affinity purify the antiserum on an HiTrap NHS-activated column (GE Healthcare Life Science).

Chloroplast fractionation and protein analysis

Immunoblot and polysome assays were performed as described earlier (Barkan, 1998). Chloroplast subfractions were those described by Williams and Barkan (2003). Stromal extract was prepared as in Watkins *et al* (2007). Sucrose gradient fractionations were performed as in Jenkins and Barkan (2001). Antisera against IM35, Cpn60 and PDH were kindly provided by Danny Schnell (University of Massachusetts), Harry Roy (Rensselaer Polytechnic Institute) and Thomas Elthon (University of Nebraska), respectively. Other antibodies were described earlier (Roy and Barkan, 1998).

RNA analyses

Analyses of RNAs that coimmunoprecipitate with PPR10 by microarray and slot-blot hybridization were performed as in Schmitz-Linneweber *et al* (2005). RNA was extracted from seedling leaves with TriZol (Gibco BRL). RNA gel blot hybridizations were performed as in Barkan (1998). For microarray profiling, 7 μg of leaf RNA from *ppr10* mutants or their normal siblings was labelled with Cy3 or Cy5, respectively, and hybridized to the microarray using the same methods as used for RIP-chip assays. Primer extension was carried out as described for poisoned primer extension (Asakura and Barkan, 2006) except that ddNTPs were not included. cRT–PCR was performed by ligating 10 μg of leaf RNA with T4 RNA ligase, followed by reverse-transcription of 5 μg of the ligated RNA using 2 pmol of primer in 20-μl reactions. The junction products were amplified by PCR (see Figure 6B). PCR products that were present in reactions involving wild type but not mutant RNA were gel purified and used as templates for PCR using primer RP1 and nested primer FP2 (Figure 6B). Products were cloned into pGEM-T and sequenced.

Generation of rPPR10

DNA encoding mature PPR10 (starting at amino acid 38) was cloned into pMAL-TEV to generate pMAL/PPR10, encoding PPR10 fused at its N terminus to MBP. Protein was expressed in *E. coli* Rosetta 2 cells (Novagen). Induction, cell lysis and amylose-affinity chromatography were as described for PPR5 (Williams-Carrier *et al*, 2008)

except that the lysis buffer contained 50 mM Tris–HCl pH 7.3, 250 mM NaCl, 1% glycerol, 0.01% CHAPS, 5 mM β-mercaptoethanol, 0.13 mM phenylmethylsulfonyl fluoride, 0.5 μg/ml leupeptin and 0.06 μg/ml pepstatin. The fusion protein was cleaved with TEV protease and resolved from MBP on a Superdex 200 column equilibrated in lysis buffer. The peak PPR10 fractions were dialyzed against 50 mM Tris–HCl pH 7.3, 250 mM NaCl, 50% glycerol, 0.01% CHAPS and 5 mM ß-mercaptoethanol, and stored at −80°C.

RNA-binding assays

GMS assays were performed as in Williams-Carrier *et al* (2008). Briefly, synthetic oligoribonucleotides were 5′-end labelled with [γ-32P]-ATP. Binding reactions contained 100 pM RNA, 200 mM NaCl, 50 mM Tris-HCl pH 7.3, 4 mM DTT, 0.1 mg/ml BSA, 10% glycerol, 10 units RNasin and 0.5 mg/ml heparin. Reactions were incubated for 30 min at room temperature and resolved on native polyacrylamide gels.

Supplementary data

Supplementary data are available at *The EMBO Journal* Online (http://www.embojournal.org).

Acknowledgements

We thank Tiffany Kroeger and Susan Belcher for identifying *ppr10* mutants, Margarita Rojas for help with protein purification, and Kenny Watkins and Rosalind Williams-Carrier for useful discussions and help preparing figures. Jeannette Pfalz was supported by a fellowship from the Deutsche Forschungsgemeinschaft. This work was supported by grants 2006-35318-17380 from the USDA-NRI and DBI-0421799 from the National Science Foundation.

Conflict of interest

The authors declare that they have no conflict of interest.

References

Asakura Y, Barkan A (2006) Arabidopsis orthologs of maize chloroplast splicing factors promote splicing of orthologous and species-specific group II introns. *Plant Physiol* **142:** 1656–1663

Barkan A (1993) Nuclear mutants of maize with defects in chloroplast polysome assembly have altered chloroplast RNA metabolism. *Plant Cell* **5:** 389–402

Barkan A (1998) Approaches to investigating nuclear genes that function in chloroplast biogenesis in land plants. *Methods Enzymol* **297:** 38–57

Barkan A, Walker M, Nolasco M, Johnson D (1994) A nuclear mutation in maize blocks the processing and translation of several chloroplast mRNAs and provides evidence for the differential translation of alternative mRNA forms. *EMBO J* **13:** 3170–3181

Beick S, Schmitz-Linneweber C, Williams-Carrier R, Jensen B, Barkan A (2008) The pentatricopeptide repeat protein PPR5 stabilizes a specific tRNA precursor in maize chloroplasts. *Mol Cell Biol* **28:** 5337–5347

Bollenbach T, Schuster G, Portnoy V, Stern D (2007) Processing, degradation, and polyadenylation of chloroplast transcripts. In *Cell and Molecular Biology of Plastids*, Bock R (ed) pp 175–211. Berlin: Springer-Verlag

Boudreau E, Nickelsen J, Lemaire S, Ossenbuhl F, Rochaix J (2000) The Nac2 gene of Chlamydomonas encodes a chloroplast TPR-like protein involved in *psbD* RNA stability. *EMBO J* **19:** 3366–3376

Cohen SN, McDowall KJ (1997) RNase E: still a wonderfully mysterious enzyme. *Mol Microbiol* **23:** 1099–1106

Condon C (2007) Maturation and degradation of RNA in bacteria. *Curr Opin Microbiol* **10:** 271–278

Deana A, Belasco JG (2005) Lost in translation: the influence of ribosomes on bacterial mRNA decay. *Genes Dev* **19:** 2526–2533

Deikus G, Condon C, Bechhofer DH (2008) Role of Bacillus subtilis RNase J1 endonuclease and 5′-exonuclease activities in trp leader RNA turnover. *J Biol Chem* **283:** 17158–17167

Drager RG, Girard-Bascou J, Choquet Y, Kindle KL, Stern DB (1998) *In vivo* evidence for 5′→3′ exoribonuclease degradation of an unstable chloroplast mRNA. *Plant J* **13:** 85–96

Drager RG, Higgs DC, Kindle KL, Stern DB (1999) 5′ to 3′ exoribonucleolytic activity is a normal component of chloroplast mRNA decay pathways. *Plant J* **19:** 521–531

Dreyfus M (2009) Killer and protective ribosomes. *Prog Nucleic Acid Res Mol Biol* **85:** 423–466

Eibl C, Zou Z, Beck A, Kim M, Mullet J, Koop HU (1999) *In vivo* analysis of plastid psbA, rbcL and rpl32 UTR elements by chloroplast transformation: tobacco plastid gene expression is controlled by modulation of transcript levels and translation efficiency. *Plant J* **19:** 333–345

Felder S, Meierhoff K, Sane AP, Meurer J, Driemel C, Plucken H, Klaff P, Stein B, Bechtold N, Westhoff P (2001) The nucleus-encoded HCF107 gene of Arabidopsis provides a link between intercistronic RNA processing and the accumulation of translation-competent psbH transcripts in chloroplasts. *Plant Cell* **13:** 2127–2141

Fisk DG, Walker MB, Barkan A (1999) Molecular cloning of the maize gene *crp1* reveals similarity between regulators of mitochondrial and chloroplast gene expression. *EMBO J* **18:** 2621–2630

Hashimoto M, Endo T, Peltier G, Tasaka M, Shikanai T (2003) A nucleus-encoded factor, CRR2, is essential for the expression of chloroplast ndhB in Arabidopsis. *Plant J* **36:** 541–549

Hirose T, Sugiura M (1997) Both RNA editing and RNA cleavage are required for translation of tobacco chloroplast *ndhD* mRNA: a possible regulatory mechanism for the expression of a chloroplast operon consisting of functionally unrelated genes. *EMBO J* **16:** 6804–6811

Hotchkiss T, Hollingsworth M (1997) RNA processing alters open reading frame stoichiometry from the large ATP synthase gene cluster of spinach chloroplasts. *Plant Mol Biol* **33:** 635–640

Jenkins B, Barkan A (2001) Recruitment of a peptidyl-tRNA hydrolase as a facilitator of group II intron splicing in chloroplasts. *EMBO J* **20:** 872–879

Lezhneva L, Meurer J (2004) The nuclear factor HCF145 affects chloroplast psaA-psaB-rps14 transcript abundance in Arabidopsis thaliana. *Plant J* **38:** 740–753

Loiselay C, Gumpel NJ, Girard-Bascou J, Watson AT, Purton S, Wollman FA, Choquet Y (2008) Molecular identification and function of cis- and trans-acting determinants for petA transcript stability in Chlamydomonas reinhardtii chloroplasts. *Mol Cell Biol* **28:** 5529–5542

Lung B, Zemann A, Madej MJ, Schuelke M, Techritz S, Ruf S, Bock R, Huttenhofer A (2006) Identification of small non-coding RNAs from mitochondria and chloroplasts. *Nucleic Acids Res* **34:** 3842–3852

Mathy N, Benard L, Pellegrini O, Daou R, Wen T, Condon C (2007) 5′-to-3′ exoribonuclease activity in bacteria: role of RNase J1 in rRNA maturation and 5′ stability of mRNA. *Cell* **129:** 681–692

Meierhoff K, Felder S, Nakamura T, Bechtold N, Schuster G (2003) HCF152, an Arabidopsis RNA binding pentatricopeptide repeat protein involved in the processing of chloroplast psbB-psbT-psbH-petB-petD RNAs. *Plant Cell* **15:** 1480–1495

Miyagi T, Kapoor S, Sugita M, Sugiura M (1998) Transcript analysis of the tobacco plastid operon rps2/atpI/H/F/A reveals the existence of a non-consensus type II (NCII) promoter upstream of the atpI coding sequence. *Mol Gen Genet* **257:** 299–307

Morin RD, Aksay G, Dolgosheina D, Ebhardt HA, Magrini V, Mardis ER, Sahinalp SC, Unrau PJ (2008) Comparative analysis of the small RNA transcriptomes of *Pinus contorta* and *Oryza sativa*. *Genome Res* **18:** 571–584

Mudd EA, Sullivan S, Gisby MF, Mironov A, Kwon CS, Chung WI, Day A (2008) A 125 kDa RNase E/G-like protein is present in plastids and is essential for chloroplast development and autotrophic growth in Arabidopsis. *J Exp Bot* **59:** 2597–2610

Murakami S, Kuehnle K, Stern DB (2005) A spontaneous tRNA suppressor of a mutation in the Chlamydomonas reinhardtii nuclear MCD1 gene required for stability of the chloroplast petD mRNA. *Nucleic Acids Res* **33:** 3372–3380

Nakamura T, Meierhoff K, Westhoff P, Schuster G (2003) RNA-binding properties of HCF152, an Arabidopsis PPR protein involved in the processing of chloroplast RNA. *Eur J Biochem* **270:** 4070–4078

Nakamura T, Sugita M (2008) A conserved DYW domain of the pentatricopeptide repeat protein possesses a novel endoribonuclease activity. *FEBS Lett* **582:** 4163–4168

Nickelsen J, Fleischmann M, Boudreau E, Rahire M, Rochaix JD (1999) Identification of cis-acting RNA leader elements required for chloroplast psbD gene expression in Chlamydomonas. *Plant Cell* **11:** 957–970

O'Toole N, Hattori M, Andres C, Iida K, Lurin C, Schmitz-Linneweber C, Sugita M, Small I (2008) On the expansion of the pentatricopeptide repeat gene family in plants. *Mol Biol Evol* **25:** 1120–1128

Rott R, Liveanu V, Drager RG, Higgs D, Stern DB, Schuster G (1999) Altering the 3 UTR endonucleolytic cleavage site of a Chlamydomonas chloroplast mRNA affects 3-end maturation *in vitro* but not *in vivo*. *Plant Mol Biol* **40:** 679–686

Roy LM, Barkan A (1998) A secY homologue is required for the elaboration of the chloroplast thylakoid membrane and for normal chloroplast gene expression. *J Cell Biol* **141:** 385–395

Sane AP, Stein B, Westhoff P (2005) The nuclear gene HCF107 encodes a membrane-associated R-TPR (RNA tetratricopeptide repeat)-containing protein involved in expression of the plastidial psbH gene in Arabidopsis. *Plant J* **42:** 720–730

Schein A, Sheffy-Levin S, Glaser F, Schuster G (2008) The RNase E/G-type endoribonuclease of higher plants is located in the chloroplast and cleaves RNA similarly to the E. coli enzyme. *RNA* **14:** 1057–1068

Schmitz-Linneweber C, Small I (2008) Pentatricopeptide repeat proteins: a socket set for organelle gene expression. *Trends Plant Sci* **13:** 663–670

Schmitz-Linneweber C, Williams-Carrier R, Barkan A (2005) RNA immunoprecipitation and microarray analysis show a chloroplast pentatricopeptide repeat protein to be associated with the 5′-region of mRNAs whose translation it activates. *Plant Cell* **17:** 2791–2804

Small I, Peeters N (2000) The PPR motif—a TPR-related motif prevalent in plant organellar proteins. *Trends Biochem Sci* **25:** 46–47

Stahl DJ, Rodermel SR, Bogorad L, Subramanian AR (1993) Co-transcription pattern of an introgressed operon in the maize chloroplast genome comprising four ATP synthase subunit genes and the ribosomal *rps2*. *Plant Mol Biol* **21:** 1069–1076

Steitz JA, Jakes K (1975) How ribosomes select initiator regions in mRNA: base pair formation between the 3′ terminus of 16S rRNA and the mRNA during initiation of protein synthesis in Escherichia coli. *Proc Natl Acad Sci USA* **72:** 4734–4738

Till B, Schmitz-Linneweber C, Williams-Carrier R, Barkan A (2001) CRS1 is a novel group II intron splicing factor that was derived from a domain of ancient origin. *RNA* **7:** 1227–1238

Tung CH, Yang JM (2007) fastSCOP: a fast web server for recognizing protein structural domains and SCOP superfamilies. *Nucleic Acids Res* **35:** W438–W443

Vaistij F, Boudreau E, Lemaire S, Goldschmidt-Clermont M, Rochaix J (2000a) Characterization of Mbb1, a nucleus-encoded tetratricopeptide repeat protein required for expression of the chloroplast *psbB/psbT/psbH* gene cluster in *Chlamydomonas reinhardtii*. *Proc Natl Acad Sci USA* **97:** 14813–14818

Vaistij FE, Goldschmidt-Clermont M, Wostrikoff K, Rochaix JD (2000b) Stability determinants in the chloroplast psbB/T/H mRNAs of Chlamydomonas reinhardtii. *Plant J* **21:** 469–482

Watkins K, Kroeger T, Cooke A, Williams-Carrier R, Friso G, Belcher S, Wijk KV, Barkan A (2007) A ribonuclease III domain protein functions in group II intron splicing in maize chloroplasts. *Plant Cell* **19:** 2606–2623

Williams P, Barkan A (2003) A chloroplast-localized PPR protein required for plastid ribosome accumulation. *Plant J* **36:** 675–686

Williams-Carrier R, Kroeger T, Barkan A (2008) Sequence-specific binding of a chloroplast pentatricopeptide repeat protein to its native group II intron ligand. *RNA* **14:** 1930–1941

Yamazaki H, Tasaka M, Shikanai T (2004) PPR motifs of the nucleus-encoded factor, PGR3, function in the selective and distinct steps of chloroplast gene expression in Arabidopsis. *Plant J* **38:** 152–163

